

**RADIOMETRIC SIMULATOR OF MAJIS ONBOARD THE JUICE MISSION: A CASE STUDY OF JUPITER HOTSPOT.** P. Haffoud<sup>1</sup>, Y. Langevin<sup>1</sup>, F. Poulet<sup>1</sup>, M. Vincendon<sup>1</sup>, A. Barbis<sup>3</sup>, J. Carter<sup>1</sup>, S. De Angelis<sup>2</sup>, M. Dexet<sup>1</sup>, C. Dumesnil<sup>1</sup>, G. Filacchione<sup>2</sup>, D. Grassi<sup>2</sup>, G. Piccioni<sup>2</sup>, C. Pilorget<sup>1</sup>, S. Rodriguez<sup>8</sup>, S. Stefani<sup>2</sup>, L. Tommasi<sup>3</sup>, F. Tosi<sup>2</sup>, <sup>1</sup>Institut d'Astrophysique Spatiale, Université Paris-Saclay, CNRS, Orsay, France (paolo.haffoud@ias.u-psud.fr), <sup>2</sup>INAF-IAPS, Frascati, <sup>3</sup>Leonardo Company, Campo-Bisenzio.

**Introduction:** MAJIS (Moons And Jupiter Imaging Spectrometer) is the visible to mid-wave infrared (0.5 to 5.56  $\mu\text{m}$ ) imaging spectrometer aboard the Jupiter Icy Moon Explorer (JUICE) [1]. JUICE is scheduled for launch in 2023. MAJIS will tour the Jovian system by performing flybys of 3 of the Galilean Moons (Callisto, Ganymede, and Europa) before getting in orbit around Ganymede. The main scientific goals of JUICE are the investigation of the emergence of habitable worlds around gas giants and the study of Jupiter as an archetype of gas giants. MAJIS will typically acquire hyperspectral data (two spatial dimensions and one spectral dimension) to quantify and map the surface composition of the Galilean Moons at various spatial resolutions, to explore their exospheres, to characterize the rings, and to monitor Jupiter's atmosphere (clouds, aerosols, aurora).

Planetary flybys (Earth/Moon and Venus) and several science planning exercises managed by the ESA/JUICE Science Operation Center are scheduled during the cruise. Radiometric simulations are essential for supporting these activities, optimizing operational parameters and generating MAJIS telecommands.

The expected signal level, as a function of the wavelength, depends on the optical efficiency of the telescope, that of the spectrometers dedicated to each channel, the transmission of the filters, and the quantum efficiency of the detectors. Early simulations during the development of MAJIS were produced using a theoretical model of the instrument. The characterization and calibration campaigns provided information of the radiometric, spectral, and spatial capabilities so that it is now possible to simulate MAJIS observations based on its measured performances.

This abstract presents updated radiometric simulations, which take into account both the outcome of the calibration campaign and the flexibility of the onboard data acquisition process.

**Derivation of the instrumental parameters:** The most extensive data set used to assess the state of the instrument and predict its performances in-flight was acquired at the Leonardo Company (Firenze) and IAS (Orsay) calibration facilities during the MAJIS calibration campaigns in 2021. This dataset includes monochromatic spectral and spatial scans, observations of black-body sources (spatially and spectrally calibrated), observations of atmospheric and gas absorption, and minerals in reflection. These

measurements acquired by MAJIS were confronted with models and previous calibration results to design an accurate instrument transfer function. These updated instrumental performances were then used as input parameters in the radiometric simulator.

**Parametrization for achieving the MAJIS science objectives:** MAJIS observations cover a vast dynamic range from very low levels (a few  $10^{-6}$  for exospheres) to levels close to saturation (Jupiter hot spots in the IR, surfaces of icy moons in the visible ranges).

Several elements have to be considered when modelling the SNR for a given observation: 1) the observational conditions (incidence, emergence, phase angle); 2) the temperatures of the optical head and focal plane units; 3) the configuration selected by TC for data processing from the detector read-out to the science data sent to the spacecraft mass memory (spatial windowing, spatial binning, frame binning, de-spiking, spectral oversampling or binning). The SNR simulations are primarily sensitive to the following parameters:

- The frame binning and de-spiking strategy have a similar impact on the SNR simulations (identified respectively by the parameters  $NPE$  and  $BIN_{DeSp}$ ). They consist of averaging several consecutive frames acquired in identical conditions.
- The spatial binning ( $BIN_{Spa}$ ), consists in averaging 2 (nominal), 4 (binning x2), or 8 (binning x8) detector rows (18- $\mu\text{m}$  wide) of the detector in the spatial direction. This increases the SNR and reduces the data volume at the expense of the spatial resolution for binning by 2 or 4 with a PSF FWHM  $\sim 36 \mu\text{m}$
- Spectral binning: A first stage of processing is performed by the proximity electronics (PE) ( $M_{PE}$  in the noise model), nominally averaging 2 physical spectels (18  $\mu\text{m}$ ). Processing independently physical spectels (oversampling) can be selected for specific wavelength ranges, with a spectral resolution improved by a factor lower than 2 due to the PSF. An additional spectral averaging x2 or x4 can also be implemented by the compression unit (CU) ( $M_{CU}$  in the noise model)

**SNR model:** A noise model was developed for the MAJIS instrument that estimates the standard deviation of the total noise of the instrument depending on the signal level measured [2]. This noise model takes into account the shot-noise and read-out noise contributions. For radiometric simulations, this noise model has been completed by taking into

account the MAJIS data flow parameters mentioned previously. This results in the following equation for the standard deviation of the total noise  $\sigma_{tot}(\lambda)$ :

$$\sigma_{tot}(\lambda) = \sqrt{\sigma_{RON}^2 \cdot M(\lambda) + IPC \cdot S_{tot}(\lambda) \cdot M(\lambda)}$$

with  $M(\lambda) = BIN_{DeSp} \cdot NPE \cdot M_{PE} \cdot M_{CU} \cdot BIN_{spa}$

where  $\sigma_{RON}$  is the read-out noise,  $IPC$  is the inter-pixel capacitance [3],  $S_{tot}(\lambda)$  the total signal (useful, dark, background) in electrons that reaches a given pixel.  $M(\lambda)$  corresponds to the total number of averaged physical pixels (18  $\mu\text{m}$ ) for each data element taking into account binning and de-spiking parameters. These parameters can be selected for up to 16 wavelength ranges for each channel, identified by dotted lines in Figure 1. Therefore, the impact of the operational parameters through the M-factor is dependent on the wavelength considered. After a check for detector saturation, the SNR is computed as the ratio of useful signal to the total noise  $\sigma_{tot}(\lambda)$ .

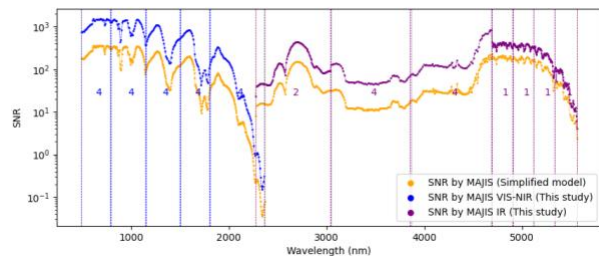


Figure 1: Comparison between expected SNR results of MAJIS when looking at Jupiter hotspots, using a simplified model (no binning or spectral editing, no de-spiking) (yellow) versus using the new model (calibration-based) developed for this study (blue and purple) and considering realistic instrumental parameters. The vertical dotted lines correspond to spectral bands. The number displayed for each spectral band is the number of physical pixels (18- $\mu\text{m}$  wide) of the detector, binned in the spectral direction.

**Results and discussion:** The test case presented here corresponds to an observation of Jupiter's atmosphere and a hot spot. Hot spots are gaps between clouds in the atmosphere of Jupiter probing deeper parts of the atmosphere that are hotter with distinctive spectral radiances close to 5  $\mu\text{m}$  ([4], [5]). The atmospheric radiance has been computed using albedo data based on measurements from the Cassini mission [6]. The hot spot radiance data has been derived from a study on the performances of two payload components of the JUNO mission [5]. In Figure 1, a comparison is made with previously available simulations, which were based on nominal processing parameters. This figure shows that in a more realistic simulation (blue and purple curve), the SNR has been significantly increased (by a factor of about 4 in the nominal spectral sampling ranges) by the frame and spatial binning parameters, and the spectral resolution adjusted from an improvement by

a factor~ 1.5 (oversampling from 4695 to 5562 nm) and a decrease by a factor of 2 (binning x2 between 3044-4695nm).

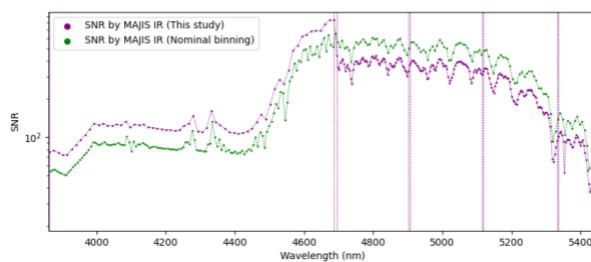


Figure 2: Comparison between "nominal" 36- $\mu\text{m}$  pixels binning (green) versus current best guess of optimized operational parameters for this study (purple).

We plan to test the impact of adjusting the other operational parameters. We will study various spectral sampling strategies depending on expected spectral signatures. As shown in Figure 2, the size and resolution of the spectral bands can be adjusted on the basis of science objectives so as to undersample spectral ranges with wide spectral signatures or oversample the spectral ranges with narrow signatures such as the thin gaseous emission lines of the hot spots around the five  $\mu\text{m}$  range ([4], [5]). Similarly, the frame binning and de-spiking will be further optimized so as to mitigate the impact of the radiative environment on data quality while preventing saturation of the detectors in spectral ranges with large radiances (thermal emissions from Jupiter, visible wavelengths for Jupiter and Galilean Moons

**Conclusion:** We have updated the SNR simulator of MAJIS. This model was used here to simulate in-flight observations of a typical Jupiter hotspot.

Other observational cases for Jupiter or the Galilean Moons will be explored for optimizing future acquisitions and generating MAJIS telecommands.

**References:** [1] Poulet F. et al (2023) *this meeting*. [2] Haffoud P. et al (2022) *Space Telescopes and Instrumentation 2022: Optical, Infrared, and Millimeter Wave*, 12180, 1168-1183. [3] Seshadri S. et al (2008) *High Energy, Optical, and Infrared Detectors for Astronomy III*, 7021, 54-64. [4] Seiff A. et al (1998) *Journal of Geophysical Research: Planets*, 103E10, 22857-22889. [5] Grassi D. et al (2010) *Planetary and Space Science*, 58(10), 1265-1278. [6] Li, L. et al (2018) *Nature Communications*, 9(1), 1-10.